IMECE2024-145950

DISTRIBUTED REAL-TIME SOIL SATURATION ASSESSMENT IN LEVEES USING A NETWORK OF WIRELESS SENSOR PACKAGES WITH CONDUCTIVITY PROBES

Puja Chowdhury
Department of
Mechanical Engineering
University of South Carolina
Columbia, South Carolina 29208
Email: pujac@email.sc.edu

James Crews
Department of
Computer Science and Engineering
University of South Carolina
Columbia, South Carolina 29208
Email: jccrews@email.sc.edu

Ayman Mokhtar
Department of Civil and
Environmental Engineering
University of South Carolina
Columbia, South Carolina 29208
Email: amokhtar@email.sc.edu

Sai Durga Rithvik Oruganti
Department of
Computer Science and Engineering
University of South Carolina
Columbia, South Carolina 29208
Email: orugants@email.sc.edu

Ryan Van Wyk
Department of
Mechanical Engineering
University of South Carolina
Columbia, South Carolina 29208
Email: rvanwyk@email.sc.edu

Austin R.J. Downey
Department of
Mechanical Engineering
Department of Civil and
Environmental Engineering
University of South Carolina
Columbia, South Carolina 29208
Email: austindowney@sc.edu

Malichi Flemming
Department of
Mechanical Engineering
University of South Carolina
Columbia, South Carolina 29208
Email: malichi@email.sc.edu

Jason D. Bakos
Department of
Computer Science and Engineering
University of South Carolina
Columbia, South Carolina 29208
Email: jbakos@cse.sc.edu

Jasim Imran
Department of Civil and
Environmental Engineering
University of South Carolina
Columbia, South Carolina 29208
Email: imran@sc.edu

Sadik Khan
Department of Civil and
Environmental Engineering
Jackson State University
Jackson, Mississippi 39217
Email: sadik.khan@jsums.edu

ABSTRACT

Levees play a critical role in safeguarding communities and assets from flooding, acting as essential defenses against the devastating impacts of inundation. Yet, earthen levees are prone to breaches, especially in the face of swift floodwaters. Distributed low-cost sensor networks offer the potential to generate spatial maps illustrating soil moisture levels. Long-term monitoring of these spatial maps could identify vulnerable zones in the levee while providing an understanding of how climate change affects levee stability. This study presents an investigation into spatial monitoring of soil saturation in levees using a wireless network of UAV-deployable sensing spike packages. The goal of this paper is to demonstrate the use of these sensors for assessing soil conductivity levels in sand-filled embankments. The obtained soil conductivity levels are crucial for determining soil saturation. The developed sensing spikes consist of a spike that penetrates the ground and measures conductivity between two electrically conductive contacts. The sensing spike consists of microprocessors for edge computing, and wireless data communication systems that report data to a way station in real-time. To validate the efficacy of the developed sensors, a flume test is developed as a replica of a levee and monitored under controlled water flow conditions. The analysis of data at different times revealed the progression of moisture throughout the earthen embankment. Initially, the soil is almost dry. As the controlled water flow proceeds, the soil becomes partially saturated, with the final stage showing a dominant presence of saturated soil. The collected data sampled at the measurement points is expanded to a continuous moisture profile using kriging. Gaussian kriging, also known as ordinary kriging, is one of the commonly used variants of the kriging method. In Gaussian kriging, the estimation of values at unsampled locations is based on a linear combination of nearby data points, with weights determined by their spatial relationships. The Gaussian assumption implies that the errors in the estimation process follow a normal distribution. The extended knowledge about saturation levels obtained through kriging can lead to insights for predicting vulnerable areas and preempting potential failures. Overall, this study paves the way for further development of a wireless network of sensing spike packages as a UAV-deployable system for levee health assessment and improved infrastructure management.

INTRODUCTION

Levees are human-made embankments, typically constructed from compacted soil and running parallel to rivers or coastlines. These elongated earthen embankments act as barriers, designed to contain overflowing water and protect adjacent land [1]. By holding back high waters, levees protect neighboring lands, including cities, infrastructure, and agricultural fields, from the devastating consequences of floods. However, levees require constant monitoring and maintenance to ensure their ef-
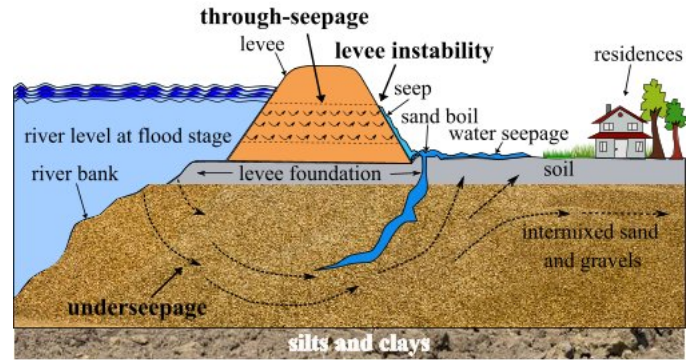

FIGURE 1. Diagram of an earthen levee depicted in cross-section, featuring labeled layers and potential areas of structural weakness.

fectiveness. To mitigate these risks, sensors can be employed for continuous monitoring, enabling early warnings for evacuation and preventative actions [2, 3]. Levee failure, the breaching of these water-containment structures, can occur due to various factors including water pressure overwhelming the structure, seepage weakening the internal foundation, and seismic activity causing structural damage [4, 5]. Internal erosion, also known as pipe erosion, weakens the levee as water seepage washes away soil particles, forming internal channels and sand boils. Animal activity and decaying root systems are identified as primary contributors to these internal pathways for water to weaken the levee and ultimately lead to its failure [6]. Figure 1, provides a detailed illustration of a levee structure.

Soil moisture monitoring is a vital component of studying soil behavior and its connection to ground movement. Soil moisture monitoring involves systematic measurement and interpretation of water within the soil. This water content directly affects how stable and prone to deformation the soil is. Researchers utilize various techniques like ground sensors, satellite data, and geophysical methods to acquire real-time data on soil moisture across various areas and timescales [7]. This information is not just beneficial for agriculture and water management, but also crucial for preventing geological hazards like landslides, subsidence, and soil erosion. By understanding the moisture levels, practitioners gain valuable insights into soil's mechanical properties [8]. This knowledge empowers engineers and geologists to predict potential ground movements and take steps to protect infrastructure and communities. Numerous published papers explore the methods, applications, and significance of soil moisture monitoring, considerably furthering geotechnical and environmental sciences [9].

Wireless sensor networks (WSNs) are powerful tools for gathering environmental data in remote or hard-to-reach locations. These networks consist of numerous small, battery-powered sensors scattered across a designated area. Each sensor collects specific data, like temperature, humidity, or soil pres-

sure, and transmits it wirelessly to a central hub. This allows for continuous monitoring over large areas without the need for cumbersome cables. WSNs are particularly advantageous for applications like precision agriculture, where they can optimize irrigation based on real-time soil moisture levels, or in environmental monitoring, where they can track air, water quality, or soil saturation levels in remote areas [10]. Their low cost, easy deployment, and minimal maintenance requirements make them a versatile technology for a wide range of applications. The emergence of compact, drone-deployable sensors offers a more cost-effective and rapid solution for assessing the health of such crucial infrastructure [11].

Spatial mapping of soil parameters is a vital tool for understanding the intricate variability of soil properties across a landscape. This technique involves collecting data on various soil characteristics, such as pH, organic matter content, or nutrient availability, at specific locations within the area of interest. By employing geostatistical techniques like kriging or regression analysis, researchers can interpolate these point measurements to create detailed maps depicting the spatial distribution of these parameters [12]. Spatial mapping aids in agriculture, land management, and environmental modeling by providing a comprehensive understanding of the intricate interplay between soil properties, like moisture levels, and other environmental factors. Published research in this field often focuses on methodological advancements and case studies demonstrating the application of spatial mapping techniques in diverse geographical settings [13].

This paper explores the spatial conductivity mapping of levees using an electric resistance-based measurement approach initially presented by the authors in Chowdhury et al. [14] that leverages rapidly deployable and open source sensors intended for levee monitoring [15]. The rapidly deployable sensors used in this work are developed for potential UAV deployment onto levees in emergency conditions [16]. In this work, a network of five independent wireless sensing spikes is used. Each handling processing, power management, sensing, and data storage. This system can help identify potential seepage points within levees, which could lead to a better understanding of maintenance needs or even levee failure. Wireless communication is used to transmit data to a way station. To map soil saturation across the levee surface, kriging is used to estimate the values between sensor locations. The results from a lab experiment are analyzed, considering both raw and interpolated data. The key contributions of this work are: (1) developing a network of wireless sensing spike packages and (2) expanding the available data through kriging and analyzing both raw data and interpolated data for measuring soil saturation levels.

METHODOLOGY

This section outlines the hardware developed for this project before presenting the experimental validations undertaken and the data processing techniques utilized.
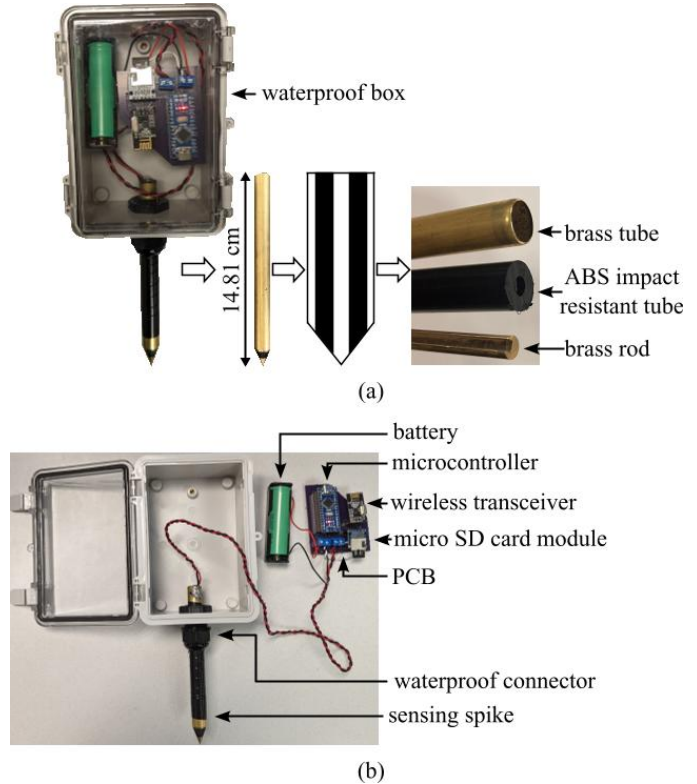

FIGURE 2. Detailed layout of a wireless sensing spike package with key components, showing: (a) outside view of the package; and (b) inside view of the package.

HARDWARE DEVELOPMENT

The hardware development phase of this work consists of two steps: 1) developing the wireless sensing spike package, and 2) wireless communications with the base station. All hardware designs used in this work are open-sourced and included in the public repository [15] under the sensor version *Mississippi* v0.1.

To simplify the wireless communication of a network of sensing spike packages, this study focused solely on the conductivity measuring aspect of the node. The sensing spike package has an instrumented spike, depicted in figure 2(a). The sensing spike has conducting surfaces - an outer tube and an inner rod - separated by an insulating ABS plastic tube. The overall length of the sensing spike is 14.81 cm. This design allows for the integration of a conductivity module into the tip of the spike, enabling the spike to also function as an underground moisture probe. Each wireless sensing spike package contains a waterproof box with PCB components and a battery. Figure 2(b), shows the inside view of the package. Waterproof connector ($\frac{1}{2}$ inch) used to harbor the sensor spike. A Samsung 25R 18650 2500 mAh 20 A battery that puts out 3.6 V to 4.2 V is used.
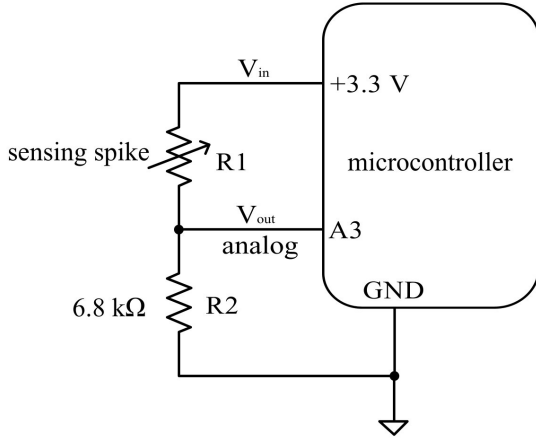
FIGURE 3. Detailed layout of the sensing spike electrical circuit for a wireless sensing spike package.

Figure 3 shows the layout for the sensing spike electric circuit. The main controller, an Arduino Nano, is accessible via headers on the PCB's front. All other components connect through the microcontroller.

To collect the data, a sensing spike is used as a resistor in a voltage divider to produce an output voltage. The +3.3 V (V_{in}) output voltage from the Arduino Nano is connected to one leg of the spike terminal (R_1), modeled as a variable resistor in the schematic. The other leg is connected to a 6.8 kΩ resistor (R_2), which is then connected to the ground. A resistor value of 6.8 kΩ is selected based on a balance between sensitivity, range, power consumption, and noise performance to ensure accurate and reliable measurement of soil conductivity or moisture level. The output voltage, the voltage divider formed by R_1 and R_2, is routed to an analog pin (A3) on the Arduino. The analog value is then converted to a digital value using the microcontroller's 10-bit analog-to-digital converter (ADC), which maps values from 0 to 1023. This digital value represents the voltage (V_{out}), which is the conductivity value targeted for wireless transmission to the base station. The voltage divider equation is in the form:

$$V_{out} = \frac{R_2}{R_1 + R_2} \cdot V_{in} \qquad (1)$$

To transmit the data, the nRF24L01+ module is used. A data packet containing the conductivity value, along with other values, is written over the network for the base station to receive.
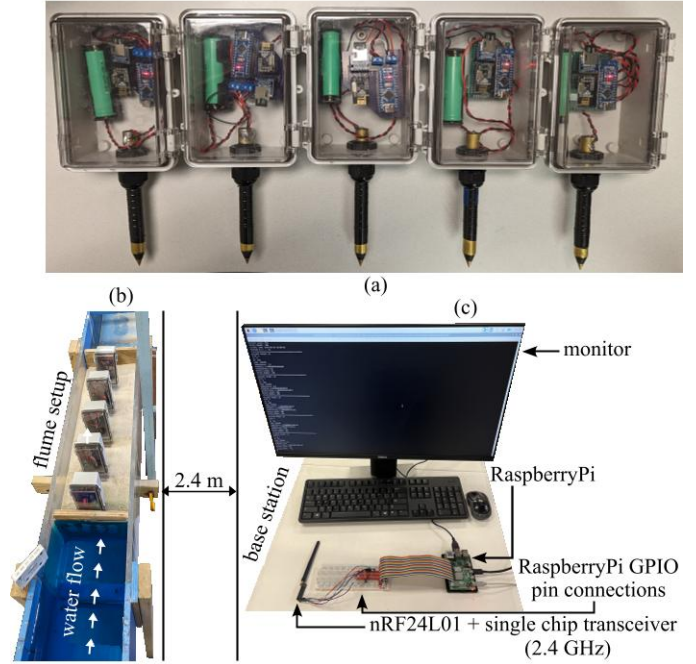

FIGURE 4. Overall wireless communication of a network of sensing spike packages, displaying: (a) network of five wireless sensing spike packages, (b) layout of the flume setup, and (c) detailed layout of the base station.

Figure 4, shows the overall wireless communication of a network of sensing spike packages. A single wireless sensing spike package as in Figure 2 reproduced for a total of five nodes. Figure 4(a) is a network of five wireless sensing spike packages. Each node must be given an address for proper communication. The RF24Network library [17] used suggests this value be in octal format or something similar (Node 1 address → 0o01, Node 2 address → 0o02, ..., etc). Figure 4(b), is the overall layout of the flume setup which is set far away (2.4 m) from the base station regarding wireless communication.

Figure 4(c), the base station must be given an address of 0o00, this is the address to which each node is transmitting data. The base station is a Raspberry Pi with an nRF24L01+ module connected. A scheduler is used to manage receiving the data from all five nodes. While all nodes are constantly sending data on a 1-second interval, the issue became clear that data may be missed from some nodes and an uneven number of data points for each node would be recorded. In an attempt to prevent this type of failure, the base station awaits to receive data from a specific node in order with a given timeout to avoid all data being compromised due to failing in a node. In a typical use case, data from node 1 is awaited until received, and then each of the nodes is iterated by following this pattern of awaiting data to be received for each node. In the case of complete failure of an individual

node, data is awaited from the node in question, a timeout is reached and the node is declared unreachable for that iteration and the sequence continues normally. When data is received by the base station it is saved to a data file specific to the node it was received from.

EXPERIMENTAL SETUP

Figure 5(a) displays the experimental setup of wireless communication for the sensing spikes for determining soil saturation levels. In the flume setup, an earthen embankment of 78 x 27 cm is used. Two wooden plates on both sides of the sand structure are used to make it stable. Figure 5(b), shows the seepage plate (left) which has small holes in the bottom that will help to propagate the water flow through the sand. The flume's height is 24 cm and is filled with sand to a height of 15 cm as shown in figure 5(d). Water is infiltrated through 5 mm holes in seepage plate (left) to simulate moisture propagation. The base station is placed around 2.4 m away from the overall flume setup as in figure 4(b) and (c). Five wireless sensing spike packages are placed in the sand as shown in figure 5(a). The main events detected during this experimental phase are the no moisture propagating and moisture propagating induced by water flow, indicated in figures 5(d) and (e). To validate the performance of the sensing spike package over time, cameras are strategically positioned on the sides and top of the experimental setup to capture the visual progression of moisture propagation.

The coordinate of the five wireless sensing spike packages is shown in table 1, where the x-coordinate represents positions along the length of the sample (78 cm), and the y-coordinate indicates positions along the width of the flume (27 cm). In this configuration, the voltage drop (V_{out}), measured as like equation 1 for each spike separately and for instance will be directly proportional to the moisture level measured by the spike (R_1) [18]. As a result, for five spike packages measured voltages are given as, $V = [v_1, v_2, \cdots, v_5]$.

TABLE 1. Coordinates for the positions of five wireless sensing spike packages in the moisture test.

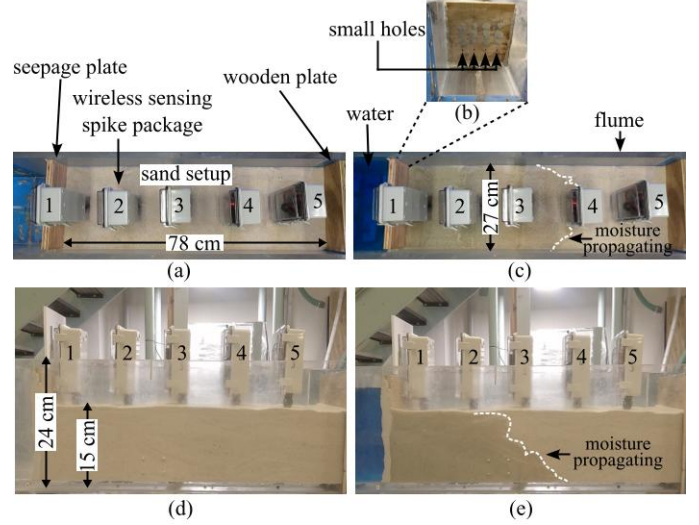| spikes	notation of fixed resistor with respect to the spike	x-coordinate (cm)	y-coordinate (cm)
1	v_1	5	13.5
2	v_2	20	13.5
3	v_3	35	13.5
4	v_4	50	13.5
5	v_5	65	13.5

FIGURE 5. Laboratory-induced setup of wireless communication for UAV-deployable sensing spikes for determining soil saturation levels of the soil with key components annotated, showing the experimental setup:(a) top view with no water flow; (b) side seepage plate (left) water flow entry; (c) top view with water flow; (d) side view with no water flow; and (e) side view with water flow.

DATA PROCESSING

To interpolate the data for all spatial points, ordinary kriging is employed [19]. The locations of the wireless sensing spike packages are denoted with corresponding coordinate $[X] = [(x_1), (x_2), \cdots, (x_5)]$. The voltage measurements are represented as $V = [v_1, v_2, \cdots, v_5]$. Given the five observations at discrete locations, the kriging model aims to accurately predict a continuous v_k at all possible x_k. The desired prediction is formulated as follows:

$$v_k = \mu + \varepsilon(x_k) \tag{2}$$

where μ denotes the true mean of the entire dataset. As the true mean value μ is unknown, estimation is performed using ordinary kriging, and $\varepsilon(\cdot)$ represents the error (small-scale variation) at x. The estimation $\hat{v}_k$ is expressed as:

$$\hat{v}_k = \sum_{i=1}^{n} \lambda_i v_i \tag{3}$$

where λ signifies the interpolation weight. Here, we assume $\lambda_1 + \lambda_2 + \lambda_3 + \lambda_4 + \lambda_5 = 1$ to yield an unbiased result. For ordinary kriging, three conditions must be met: 1) linearity ($\hat{v}_k = \sum_{i=1}^{n} \lambda_i v_i$), 2) unbiasedness ($\sum_{i=1}^{n} \lambda_i = 1$), and 3) minimized error: selecting the most appropriate values for the coefficients
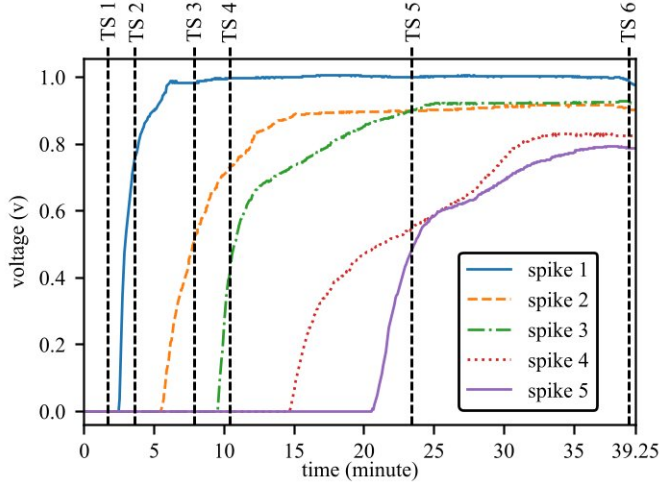
FIGURE 6. Data obtained from five wireless sensing spike packages during the overall moisture test. The Black dashed line indicates six-time stamps TS 1 - TS 6.

λ_n and the Lagrange multiplier $2m$. E denotes the estimated function [19]. Consequently, the loss function for the problem is defined as:

$$L_{\text{kriging}} = E\left(v_k - \sum_{i=1}^{n} \lambda_i v_i\right) - 2m\left(\sum_{i=1}^{n} \lambda_i - 1\right) \quad (4)$$

The PyKrige library is used to perform the kriging process [20]. The data containing sensor locations, and voltage readings [X, V] is used to train the Gaussian variogram models. For this study, a simple boolean operator is implemented to the estimated voltage, wherein any inferred voltage values below zero are adjusted to zero ($V < 0 \rightarrow 0$), reflecting the fact that negative voltage readings are not physically feasible.

RESULTS AND DISCUSSION

The overall results of the moisture test conducted using the network of five wireless sensing spike packages are illustrated in Figure 6. The duration of this test spans approximately 2355 s (39.25 minutes). The figure depicts how the voltage of each sensing spike gradually increases over time. As previously mentioned, the measured voltage is proportional to the moisture level detected by the sensing spike. For a comprehensive analysis, six different timestamps (TS) throughout the entire test are considered: 100, 216, 472, 624, 1402, and 2339 s.

Figure 7 presents the side view for TS 1, TS 2, TS 3, TS 4, TS 5, and TS 6 consecutively. At TS 1 (around 100 s), minimal moisture propagation is observed, as shown in Figure 7(a). Experimental illustrations for other timestamps, namely TS 2 through TS 6, are shown in figures 7(b) through 7(f).
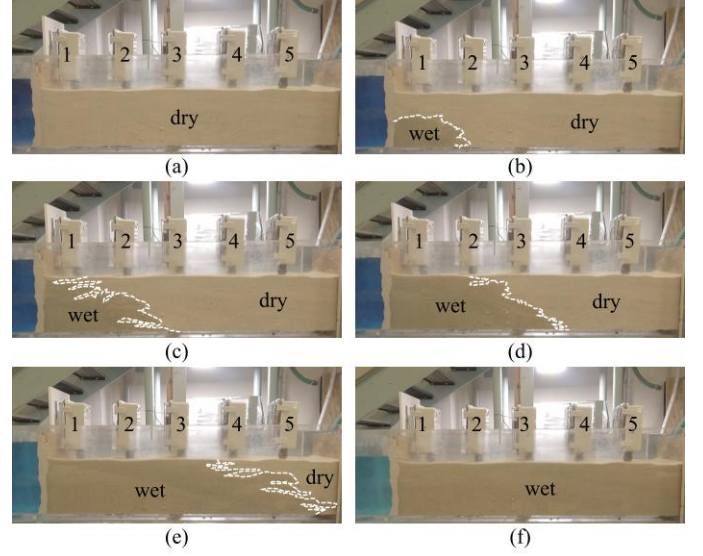

FIGURE 7. The experimental configuration illustrating the locations of five wireless sensing spike packages as moisture spreads, including (a) side view at TS 1; (b) side view at TS 2; (c) side view at TS 3; (d) side view at TS 4; (e) side view at TS 5; and (f) side view at TS 6.

TABLE 2. Voltage (V) measurements for the five wireless sensing spike packages at TS.

			voltage (V)				
			spike 1	spike 2	spike 3	spike 4	spike 5
time stamp (s)	TS 1	100	0.000	0.000	0.000	0.000	0.000
	TS 2	216	0.751	0.000	0.000	0.000	0.000
	TS 3	472	0.983	0.519	0.000	0.000	0.000
	TS 4	624	0.996	0.729	0.416	0.000	0.000
	TS 5	1402	1 .000	0.900	0.9 00	0.545	0.477
	TS 6	2339	0.987	0.906	0.925	0.825	0.787

Table 2 displays the voltage measurements for the five wireless sensing spike packages at TS. In the second time measurement (TS 2), only spike 1 recorded a voltage reading of around 0.751 V . This suggests that moisture is mainly moving through spike 1 at this point, as shown in figure 7(b). At TS 4, moisture propagates through spikes 1, 2, and 3. In the cases of TS 5 and TS 6, moisture propagates across all wireless five sensing spike packages.

As all 5 sensing spike packages are in a line, figure 8 shows overall 1D kriging outcomes from the moisture test for six different timestamps in case of y-axis location (denoted as location). From table 2, minimal moisture is observed and voltage measurement is zero at TS 1. So the moisture mapping as figure 8 shows the lowest amount of moisture in almost the overall area for TS 1. In the case of TS 4 from figure 7(d), spikes 1, 2, and
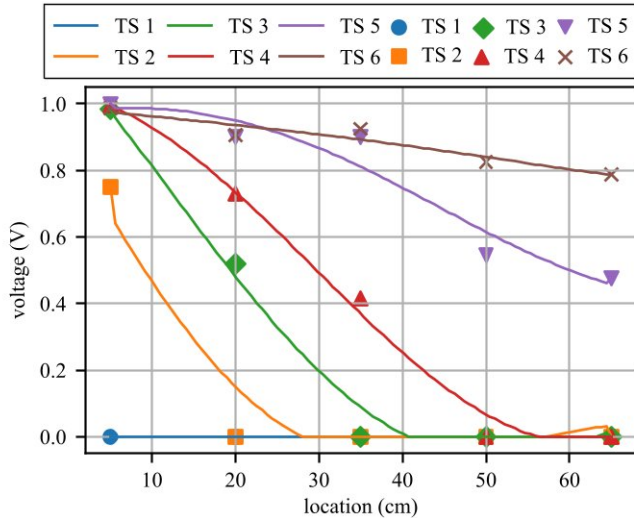
6

FIGURE 8. 1D kriging outcomes from the moisture test for six-TS.

3 show a gradually increasing amount of voltage change concerning the moisture level of propagation. This correlates to the moisture map produced by the kriging algorithm shown in figure 8. At TS 5 shown in figure 7(e), the entire test volume shows evidence of water propagation as does the kriging inferred results for TS 5 in figure 8. Lastly, TS 6 which correlates to figure 7(f) shows nearly complete soil saturation.

CONCLUSION

This study demonstrated the potential of wireless communication for a network of sensing spike packages for levee monitoring. The experiment employed these packages embedded in a laboratory setting to measure soil conductivity and assess moisture levels. By combining kriging for data interpolation and preliminary data analysis, the research mapped soil saturation across the levee. The analysis of data from six different time stamps revealed the progression of moisture throughout the simulated levee. Initially, the soil was almost dry. As the controlled water flow proceeded, the area became progressively saturated, with the final stage showing a dominant presence of partially saturated soil. This information provides valuable insights for monitoring real-world levees and identifying potential areas of concern for maintenance or preventative measures.

Overall, this initial study paves the way for further development of a wireless network of sensing spike packages as a rapidity-deployable system for levee health assessment. The ability to measure soil conductivity and analyze saturation levels offers a promising approach for proactive levee monitoring and improved infrastructure management.

REFERENCES

[1] Tsai, C.-C., Yang, Z.-X., Chung, M.-H., and Hsu, S.-Y., 2022. "Case study of large-scale levee failures induced by cyclic softening of clay during the 2016 meinong earthquake". *Engineering Geology, 297*, p. 106518.

[2] Radzicki, K., Gołębiowski, T., Ćwiklik, M., and Stoliński, M., 2021. "A new levee control system based on geotechnical and geophysical surveys including active thermal sensing: A case study from poland". *Engineering Geology, 293*, p. 106316.

[3] Cola, S., Girardi, V., Bersan, S., Simonini, P., Schenato, L., and De Polo, F., 2021. "An optical fiber-based monitoring system to study the seepage flow below the landside toe of a river levee". *Journal of Civil Structural Health Monitoring, 11*(3), pp. 691–705.

[4] Orlandini, S., Moretti, G., and Albertson, J. D., 2015. "Evidence of an emerging levee failure mechanism causing disastrous floods in i taly". *Water Resources Research, 51*(10), pp. 7995–8011.

[5] Rapti, I., Lopez-Caballero, F., Modaressi-Farahmand-Razavi, A., Foucault, A., and Voldoire, F., 2018. "Liquefaction analysis and damage evaluation of embankment-type structures". *Acta Geotechnica, 13*(5), pp. 1041–1059.

[6] Camici, S., Barbetta, S., and Moramarco, T., 2017. "Levee body vulnerability to seepage: The case study of the levee failure along the foenna stream on 1 january 2006 (central italy)". *Journal of Flood Risk Management, 10*(3), pp. 314–325.

[7] SU, S. L., Singh, D. N., and Baghini, M. S., 2014. "A critical review of soil moisture measurement". *Measurement, 54*, pp. 92–105.

[8] Das, B. M., 2019. *Advanced soil mechanics*. CRC press.

[9] Leone, M., 2022. "Advances in fiber optic sensors for soil moisture monitoring: A review". *Results in Optics, 7*, p. 100213.

[10] Lloret, J., Sendra, S., Garcia, L., and Jimenez, J. M., 2021. "A wireless sensor network deployment for soil moisture monitoring in precision agriculture". *Sensors, 21*(21), p. 7243.

[11] Zwęgliński, T., 2020. "The use of drones in disaster aerial needs reconnaissance and damage assessment – three-dimensional modeling and orthophoto map study". *Sustainability,* *12*(15), jul, p. 6080.

[12] Conforti, M., Matteucci, G., and Buttafuoco, G., 2017. "Organic carbon and total nitrogen topsoil stocks, bio-genetic natural reserve 'marchesale'(calabria region, southern italy)". *Journal of Maps,* *13*(2), pp. 91–99.

[13] Garg, P. K., Garg, R. D., Shukla, G., and Srivastava, H. S., 2020. "Digital mapping of soil landscape parameters". *Poland: Springer International Publishing*.

[14] Chowdhury, P., Satme, J. N., Yount, R., Downey, A. R., Khan, S., Imran, J., and Micheli, L., 2023. "Classifying soil saturation levels using a network of uav-deployed smart penetrometers". In Smart Materials, Adaptive Structures and Intelligent Systems, Vol. 87523, American Society of Mechanical Engineers, p. V001T05A002.

[15] Flemming, M., and Downey, A. Smart penetrometer with edge computing and intelligent embedded systems. GitHub.

[16] Chowdhury, P., Satme, J. N., Flemming, M., Downey, A. R., Elkholy, M., Imran, J., and Khan, M. S., 2023. "Stand-alone geophone monitoring system for earthen levees". In Sensors and Smart Structures Technologies for Civil, Mechanical, and Aerospace Systems 2023, Vol. 12486, SPIE, pp. 168–174.

[17] RF24Network Development Team, Year of last update, e.g., 2022. RF24Network Documentation. Accessed on current date, e.g., May 3, 2024.

[18] Murad, O. F., et al., 2012. "Obtaining chemical properties through soil electrical resistivity". *Journal of Civil Engineering Research,* *2*(6), pp. 120–128.

[19] Rouhani, S., and Wackernagel, H., 1990. "Multivariate geostatistical approach to space-time data analysis". *Water Resources Research,* *26*(4), pp. 585–591.

[20] GeoStat-Framework. Pykrige documentation. Downloaded from https://geostat-framework.readthedocs.io/_/downloads/pykrige/en/v1.5.0/pdf/. Version 1.5.0.